Translocation and Clustering of Endosomes and Lysosomes Depends on Microtubules

Raffaele Matteoni and Thomas E. Kreis

European Molecular Biology Laboratory, D-6900 Heidelberg, Federal Republic of Germany

Abstract. Indirect immunofluorescence labeling of normal rat kidney (NRK) cells with antibodies recognizing a lysosomal glycoprotein (LGP 120; Lewis, V., S. A. Green, M. Marsh, P. Vihko, A. Helenius, and I. Mellman, 1985, *J. Cell Biol.*, 100:1839–1847) reveals that lysosomes accumulate in the region around the microtubule-organizing center (MTOC). This clustering of lysosomes depends on microtubules. When the interphase microtubules are depolymerized by treatment of the cells with nocodazole or during mitosis, the lysosomes disperse throughout the cytoplasm. Lysosomes recluster rapidly (within 30–60 min) in the region of the centrosomes either upon removal of the drug, or, in telophase, when repolymerization of interphase microtubules has occurred. During this translocation process the lysosomes can be found aligned along centrosomal microtubules.

Endosomes and lysosomes can be visualized by incubating living cells with acridine orange. We have

analyzed the movement of these labeled endocytic organelles in vivo by video-enhanced fluorescence microscopy. Translocation of endosomes and lysosomes occurs along linear tracks (up to 10 μm long) by discontinuous saltations (with velocities of up to 2.5 μm/s). Organelles move bidirectionally with respect to the MTOC. This movement ceases when microtubules are depolymerized by treatment of the cells with nocodazole. After nocodazole washout and microtubule repolymerization, the translocation and reclustering of fluorescent organelles predominantly occurs in a unidirectional manner towards the area of the MTOC. Organelle movement remains unaffected when cells are treated with cytochalasin D, or when the collapse of intermediate filaments is induced by microinjected monoclonal antivimentin antibodies. It can be concluded that translocation of endosomes and lysosomes occurs along microtubules and is independent of the intermediate filament and microfilament networks.

LIGANDS bound to specific receptors on the plasma membrane are internalized by the cell via receptor-mediated endocytosis. During this process receptor-ligand complexes are found sequentially in coated pits, coated vesicles, and endosomes, where some ligands dissociate from their receptors and the latter recycle back to the plasma membrane. Remaining complexes and dissociated ligands are then delivered to lysosomes (for reviews see 17, 19, 22, 34, 40, 49). Cytoskeletal structures appear to be required for the delivery of internalized surface components to the lysosomes (7, 21, 27, 38). So far very little is known about the mechanisms for sorting membrane components and internalized material during endocytosis. Increasing organelle acidity concomitant with the delivery of endocytosed material from coated vesicles to endosomes and finally to the lysosomes may play an important role in this sorting process (35, 36). Whether or not the cytoskeleton is involved in the routing of endocytic organelles during the sorting of internalized material remains an important question.

The movement of endocytic organelles has been visualized in vivo by light microscopy using phase-contrast (13, 21, 31), darkfield (58), and video-intensified fluorescence (21, 57). These approaches have shown that the organelles move in a discontinuous, nonBrownian fashion, referred to as saltatory movement (42). Vesicle formation has been observed to take place at the cell periphery, and vesicles have been shown to preferentially exhibit centripetal migration (13, 21, 31, 55). Treatment of cells with various cytoskeleton-disrupting drugs revealed the involvement of the cytoskeleton in the translocation of endocytic vesicles. It was suggested that microtubules were important for the movement of these organelles (13, 21, 41); an active role for microfilaments and intermediate filaments was also proposed (20, 41, 52).

The aim of this study was to further analyze the role of cytoskeletal structures in the translocation and positioning of endosomes and lysosomes in fibroblasts. Vital fluorescence staining of these endocytic organelles and the application of video-enhanced fluorescence microscopy (VEFM)[1] allowed

---

1. *Abbreviations used in this paper:* AO, acridine orange; fl-TFG, fluorescein-labeled transferrin-gold complexes; glu-tubulin, detyrosinated α-tubu-

the dynamic interactions of these organelles within the cytoskeletal network to be investigated. The data obtained suggest that the movement of endosomes and lysosomes and their final accumulation in clusters in the perinuclear region of the microtubule organizing center (MTOC) requires an intact microtubule framework, but is independent of microfilaments and intermediate filaments.

Materials and Methods

Cell Culture and Drug Treatment of Cells

Normal rat kidney (NRK) cells were grown in MEM containing 10% FCS, 1% nonessential amino acids, 1% penicillin and streptomycin, and 1% L-glutamine (culture medium). For immunofluorescence, microinjection, and in vivo labeling experiments, cells were grown on glass coverslips and used 24–30 h after plating.

The depolymerization of microtubules or microfilaments was achieved by incubation of the cells in culture medium containing 10 µM nocodazole (Sigma Chemical Co., St. Louis, MO) for 5 h or 1 µM cytochalasin D (Calbiochem-Behring Corp., La Jolla, CA) for 1 h, both at 37°C. Nocodazole treatment was followed in some experiments by three washes with, and incubation in, nocodazole-free culture medium. Nocodazole was stored at −20°C as a 10-mM stock solution in DMSO. Aliquots were thawed immediately before use and appropriately diluted with culture medium.

Labeling of Endocytic Organelles

Acidic organelles of living NRK cells were fluorescently labeled with acridine orange (AO) (Calbiochem-Behring Corp.) Cells on coverslips were rinsed with Hank's balanced salt solution containing 2 mg/ml BSA (H-BSA) and then incubated for 1 min at room temperature in H-BSA containing 20 µM AO. This short incubation was sufficient to allow the weak base AO to partition into the lumen of acidic organelles and to accumulate as the protonated, fluorescent molecule. A fresh stock solution of AO (2 mM) in water was prepared immediately before use. Excess AO was removed by washing the cells with H-BSA for 2.5 min. The coverslips were then used for fluorescence visualization.

Endocytic organelles were also labeled in vivo with fluorescently labeled transferrin complexed with 12 nm colloidal gold (fl-TFG). Fl-TFG was prepared as follows. Human or rat transferrin-gold (kindly provided by Dr. G. Griffiths, European Molecular Biology Laboratory, Heidelberg, Federal Republic of Germany) was made to 35 µM in PBS, containing 100 mM Tris-HCl, pH 7.4, and modified with 700 µM 6-iodoacetamido-fluorescein (Molecular Probes, Inc., Junction City, OR) for 15 min at room temperature. Free fluorochrome was removed by chromatography over a Sephadex G-50 column (Pharmacia, Uppsala, Sweden) equilibrated with PBS. Then 200 mM NaHCO₃, pH 8.5, was added and further labeling for 15 min at room temperature was performed with 700 µM 5-(4,6-dichlorotriazinyl) aminofluorescein (Molecular Probes, Inc.). The reaction was quenched with 10 mM glycine, pH 8.5, for 10 min at room temperature and free fluorochrome was removed by gel filtration as described above. TFG was labeled with both the sulfhydril- and the primary amino-reactive fluorescein derivative to obtain maximal labeling. The final molar ratio of fluorochrome to protein was 1.5. The labeled protein was free of uncovalently bound fluorochrome as judged by SDS-PAGE. Cells on coverslips were deprived of endogenous transferrin by incubation in serum-free culture medium containing 2 mg/ml BSA for 1 h at 37°C. Subsequently, fl-TFG (1.5 mg/ml) in serum-free culture medium supplemented with 2 mg/ml BSA was added to the cells for 30 min at 19.5°C. After a 15-min chase at 19.5°C in transferrin- and serum-free medium containing BSA, cells on coverslips were rinsed with H-BSA either immediately at 19.5°C, or after 1 h incubation at 37°C in serum-free medium. The labeled cells on coverslips were then used for fluorescence visualization. Binding of fl-TFG was essentially blocked at 4°C by 20-fold excess of free transferrin.

Cells grown on round glass coverslips with a diameter of 22 mm were mounted into a stainless steel thermostatic chamber for visualization by VEFM. The external jacket of the chamber was connected to a thermostat

---

lin; H-BSA, Hank's balanced salt solution supplemented with 2 mg/ml BSA; MTOC, microtubule-organizing center; VEFM, video-enhanced fluorescence microscopy.

JULABO F 10-UC (JULABO Labortechnik, Seelback, FRG), allowing continuous circulation of a thermostatic fluid at constant temperature within the range of −20–60°C. The temperature of the medium in the chamber was monitored by a temperature sensor.

Immunofluorescence

Double immunofluorescence staining of lysosomes and microtubules was carried out according to either of two different protocols. (a) Cells were fixed in 3% paraformaldehyde/0.02% glutaraldehyde in PBS and permeabilized in methanol at −20°C as described (32). Lysosomes and microtubules were labeled using rabbit antibodies against a 120K lysosomal membrane glycoprotein (anti-LGP120; 32), and a rat monoclonal antibody against tubulin (YL1/2; 24). (b) Cells were fixed and extracted in methanol for 5 min at −20°C for double immunofluorescence labeling of lysosomes using a murine monoclonal antibody against the 120K lysosomal membrane protein (Ly1C6; 32), and microtubules containing predominantly detyrosinated α-tubulin subunits (glu-tubulin) using affinity-purified rabbit antibodies specific for glu-tubulin (anti-glu-tubulin) (30a).

Goat anti-rabbit, goat anti-mouse, and goat anti-rat, coupled with fluorescein or rhodamine, were used as second antibodies as described previously (30). Both rabbit anti-LGP120 and the mouse Ly1C6 monoclonal antibody were provided by Dr. I. Mellman (Yale University, New Haven, CT); the rat monoclonal YL1/2 anti-tubulin was obtained from Dr. J. Kilmartin (Medical Research Council, Cambridge, United Kingdom).

Cells were also fixed and extracted in methanol according to protocol b for immunolabeling with human autoimmune antiserum against centriolar antigens (51). Antibodies against centrosomes and fluorescein-labeled goat anti-human antibodies were both obtained from Dr. M. Kirschner (University of California, San Francisco, CA).

In some experiments cells were fixed immediately after visualization in vivo of fluorescently labeled organelles by perfusing the thermostatic chamber with the mixture of paraformaldehyde and glutaraldehyde as described above (protocol a). The field containing the observed cells was marked by scratching the glass, which allowed orientation of the coverslip with respect to the axis of the microscope stage. The coverslip was then removed from the chamber and immunofluorescence labeling of lysosomes and microtubules was performed as described above.

Conventional fluorescence microscopy and photography with fixed and immunolabeled samples were performed as described, using a Zeiss photomicroscope III (29).

VEFM and Tracking of Organelle Movement

Movement of fluorescently labeled organelles was visualized in vivo by VEFM. The following combinations of filter sets were used for fluorescence microscopy: the N2.1 filter set for rhodamine (BP 515-560, RKP 580, LP 580) and the L2 filter set for fluorescein (BP 450-500, RKP 510, BP 515-560). To avoid the diffuse background of AO in the cytoplasm visible in the fluorescein filter set we monitored AO-labeled organelles using the rhodamine filter set. An ISIT-66 camera (Dage-MTI Inc., Michigan City, IN) was connected by a 0.5–6.25× zoom (Leitz, Stuttgart, FRG) to a Leitz Diavert inverted fluorescence microscope. The signal from the ISIT camera was enhanced by an Image Σ real time image processor (Nippon Avionics, Tokyo, Japan). For processing of the input image we applied recursive filtering by means of the averaging algorithm of the processing unit, according to the formula $M_f = k^{-1} \cdot L + (1 - k^{-1}) \cdot M_i$. M_f is the final image stored after processing, L the unprocessed input image, M_i the stored image at a given time, and k the sampling constant corresponding to a given number of frames. The averaging process results in an increased signal to noise ratio by a factor $I = \sqrt{(2k - 1)}$. For the visualization of organelle movement we used a constant value for k of 128 frames. Periods of illumination of the labeled cells were controlled by an electronic shutter system connected to an iris that was inserted into the optical path of the fluorescence excitation light. The intensity of the fluorescence excitation light was reduced (usually 1024-fold) by neutral density filters (Leitz). These low light levels allowed continuous recording of fluorescently labeled cells for more than 30 min without significant alterations to the pattern of organelle motility. The processed image was recorded onto National NV-P76H video tape (Panasonic, Hamburg, FRG) by a National NV-8030 time-lapse video tape recorder (Panasonic) and monitored in parallel on a Panasonic WV-5350 video monitor. Photographs of the recorded images were taken with a Polaroid camera from the video monitor onto positive-negative film (model 665).
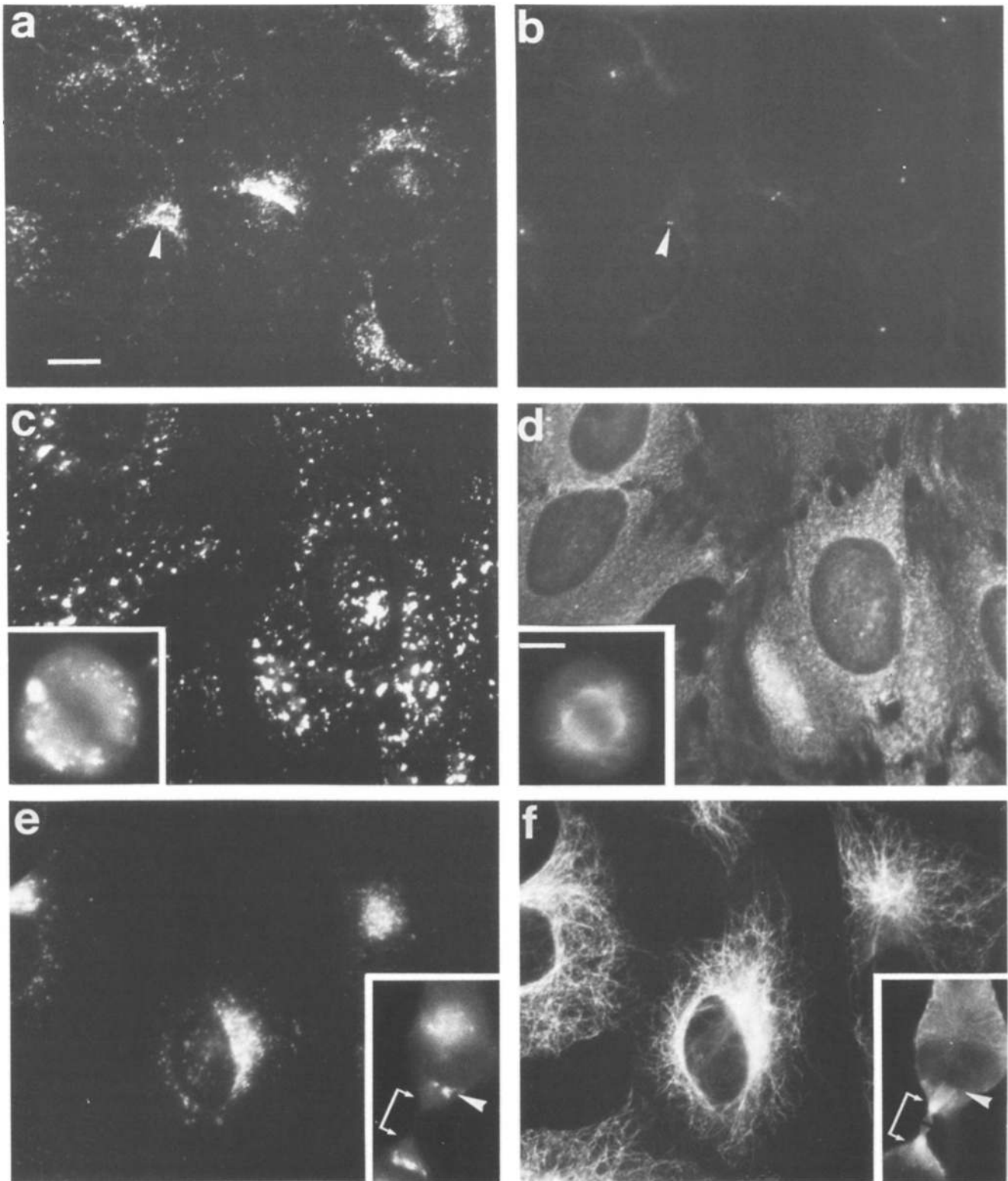
Figure 1. Microtubule-dependent clustering of lysosomes in the area of centrosomes. Lysosomes (*a*, *c*, and *e*) and centrosomes (*b*) or microtubules (*d* and *f*) were visualized in NRK cells by double immunofluorescence labeling with specific antibodies (for details see Materials and Methods). Identical cells are shown in *a* and *b*, *c* and *d*, and *e* and *f*. The arrowheads in *a* and *b* point to a typical cluster of lysosomes in the region of the centrosome in untreated cells. Treatment of NRK cells with 10 μM nocodazole for 5 h completely depolymerized the interphase microtubules (*d*) and induced scattering of the lysosomes throughout the cytoplasm (*c*). Untreated cells in metaphase are shown in the insets (*c* and *d*). Microtubules repolymerized after subsequent incubation of nocodazole-treated cells for 1 h in normal culture medium without the drug (*f*) and lysosomes reclustered in the region of the MTOC (*e*). In untreated NRK cells in telophase (insets in *e* and *f*) lysosomes clustered at the distal ends of the midbody microtubules (*arrowheads*) and around newly formed MTOCs, but they were absent from the midbody region (*double arrow*). Bars: (*a–f*) 10 μm; (insets) 5 μm.

The movement of the fluorescently labeled organelles was recorded by VEFM. Tracks of the movement of individual organelles were transferred by manual tracing onto transparent acetate sheets attached to the video monitor during playback of the recorded videotapes.

Microinjection

An IgG fraction (3 mg/ml) of a monoclonal antibody against vimentin (7A3), was microinjected into NRK cells. Microinjection was performed as described elsewhere (28, 30). Cells were maintained in culture medium for 6 h postinjection and subsequently processed for drug treatment and immunofluorescence labeling as described above.

For in vivo visualization cells were microinjected with rhodamine-labeled 7A3 (0.75 mg/ml). Rhodamine labeling of the antibody was carried out as described (30). The distribution of injected rhodamine-labeled antibody was recorded by VEFM before staining of the organelles with AO and tracking of their movements.

Results

Clustering of Lysosomes in the Area of the Centrosome Depends on Microtubules

Immunofluorescence labeling of interphase NRK cells with anti-LGP120, recognizing a specific lysosomal membrane antigen (32), revealed the perinuclear accumulation of most of the lysosomes (Fig. 1). Double immunolabeling with anti-centrosome antibodies (Fig. 1 b) indicated that the lysosomes clustered in the area of the MTOC (Fig. 1 a). The Golgi apparatus was localized in this same region when immunolabeled with an antibody recognizing a cytoplasmic Golgi membrane–associated 110K protein (2) but the two compartments did not overlap (data not shown). The lysosomes in metaphase cells were usually randomly scattered (insets in Fig. 1, c and d). In telophase they reclustered in the centrosomal area of the two daughter cells and clusters of lysosomes were also consistently observed at the distal ends of the midbody microtubules (insets in Fig. 1, e and f).

Lysosomes became scattered in the cytoplasm when interphase microtubules were completely depolymerized by treatment of NRK cells for 5 h with 10 µM nocodazole (Fig. 1, c and d). Lysosomes were randomly distributed in the cytoplasm in >90% of these cells, whereas in the absence of the drug ~80% of the cells exhibited clustered lysosomes (Table I). Lysosomes rapidly reclustered in the centrosomal region when cells with depolymerized microtubules were transferred to normal culture medium without nocodazole (Fig. 1, e and f). Within 60 min >90% of the cells contained a distinct centrosomal cluster of lysosomes (Table I and Fig. 2).

Table I. Clustering of Lysosomes Depends on the Organization of Microtubules

Treatment of NRK cells	Cells containing lysosome clusters	Average No. of lysosome clusters per cell (SD)
	%	
Normal culture medium	79.2	0.9 (0.5)
10 µM nocodazole for 5 h	8.2	0.1 (0.3)
10 µM nocodazole for 5 h followed by incubation in normal culture medium for 1 h	93.7	1.0 (0.2)

Clustering of lysosomes after drug treatment was analyzed in cells labeled for immunofluorescence microscopy with specific antibodies as described in the legend to Fig. 1. For each assay 500 cells were analyzed. Typical cells with clustered or spread lysosomes are shown in Fig. 1.

This reclustering began when the microtubules had repolymerized to an average length that exceeded the mean distance from the MTOC to the cell periphery (see Fig. 2). Therefore, the accumulation of lysosomes in the region of the MTOC clearly depends on the presence of microtubules.

Association of Lysosomes with Centrosome-nucleated Microtubules

The association of lysosomes with microtubules during reclustering after removal of nocodazole was analyzed by indirect immunofluorescence labeling (Fig. 3). The rate of microtubule repolymerization was reduced by incubating the drug-treated cells in medium containing low concentrations of nocodazole (0.02–0.1 µM). In such cells lysosomes were often seen aligned along distinct centrosome-nucleated microtubules (Fig. 3, a–d). The distribution of these aligned lysosomes resembled the pattern of short centrosome-nucleated microtubule asters (Fig. 3, c, e, and f). Such an alignment of lysosomes was also detected, albeit more rarely, in untreated NRK cells (Fig. 4 a). Occasionally lysosomes were found associated with non–centrosome-nucleated microtubules (Fig. 3 g, corresponding microtubule staining not shown), which emanated from foci not overlapping with the centrosome area (data not shown). Control experiments revealed that the antilysosome serum did not stain any cytoskeletal structures (data not shown, see also Fig. 1 a).

The alignment of lysosomes appeared to occur rather selectively along a subset of microtubules. To investigate whether alignment of lysosomes occurred along the subset of interphase microtubules predominantly containing glu-tubulin (18), double-labeling with murine Ly1C6 (32) and rabbit anti–glu-tubulin was performed. Lysosomes did not align along the microtubules heavily labeled by anti–glu-tubulin (Fig. 4). Furthermore, within 30 min after nocodazole washout >50% of NRK cells had clustered lysosomes (Fig. 2), but no labeling of microtubules with anti–glu-
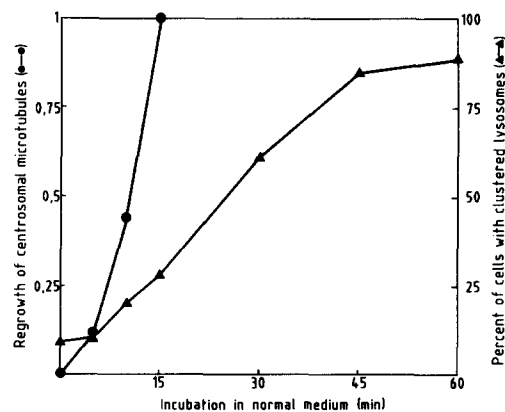

Figure 2. Clustering of lysosomes depends on the presence of microtubules. Cells were treated with nocodazole as described in Fig. 1 and subsequently transferred to normal culture medium. At the indicated time points after nocodazole washout cells were fixed and double-labeled with antilysosome and antitubulin antibodies. The number of cells out of 20 containing clustered lysosomes was counted and the average length of repolymerized centrosome-nucleated microtubules measured. The index for microtubule regrowth was calculated by dividing the average microtubule length by the average maximal distance between the centrosomal area and the cell periphery (29 ± 7 µm).
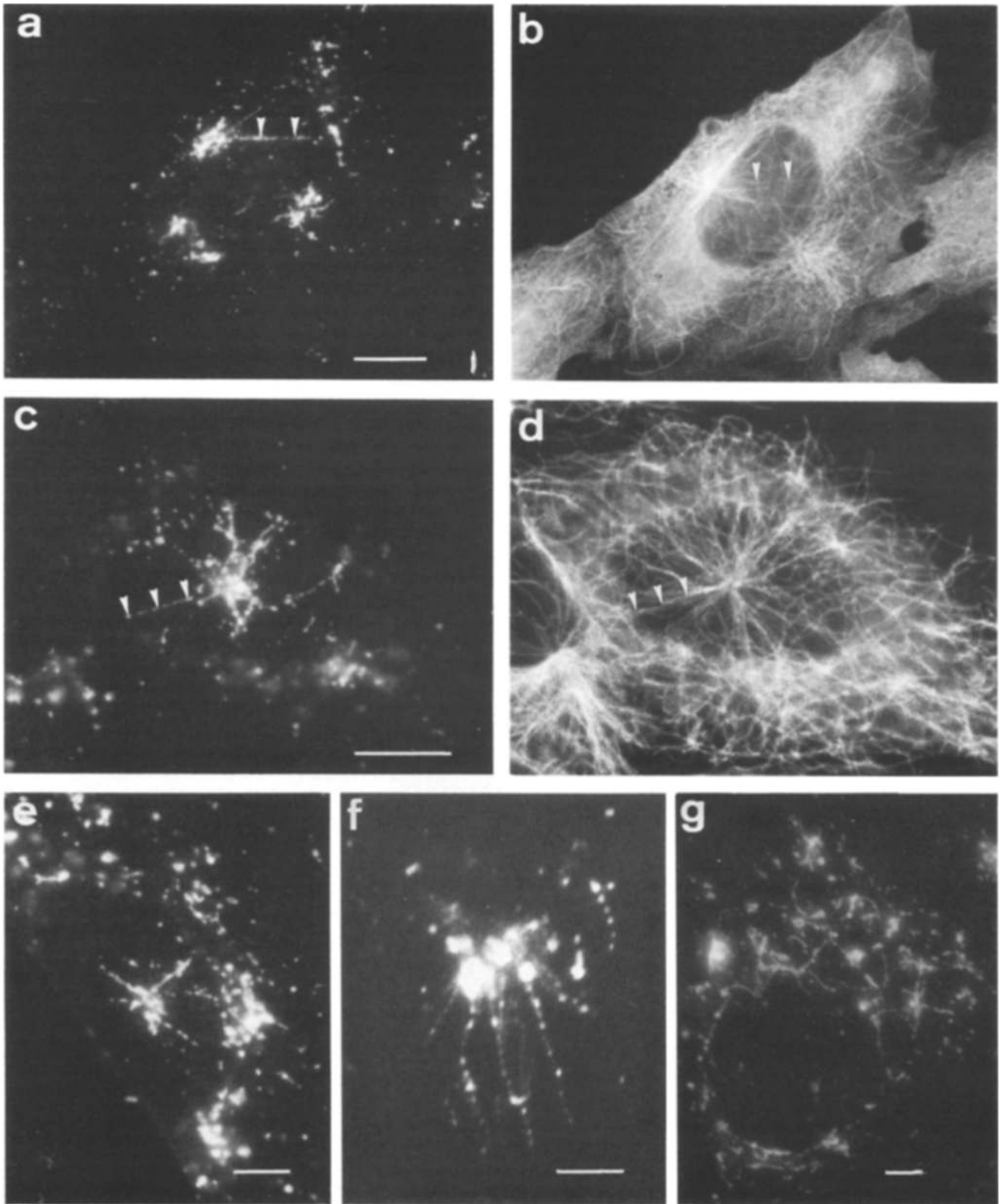
Figure 3. Alignment of lysosomes along centrosomal microtubules during reclustering. NRK cells were incubated for 4 h in medium containing 1 μM nocodazole to disassemble microtubules. They were subsequently transferred to medium containing 0.02 μM nocodazole (*c*, *d*, and *e*), or 0.1 μM nocodazole (*a*, *b*, *f*, and *g*) and fixed after 5 min (*a–e* and *g*) or 30 min (*f*). Double immunofluorescence staining was carried out using antilysosome (*a*, *c*, *e*, *f*, and *g*) and antitubulin (*b* and *d*) antibodies. Arrowheads indicate linear arrays of lysosomes along centrosome-nucleated microtubules. Association of lysosomes appeared to occur with a distinct subset of microtubules (*b* and *d*). Bars: (*a–d*) 10 μm; (*e–f*) 5 μm.
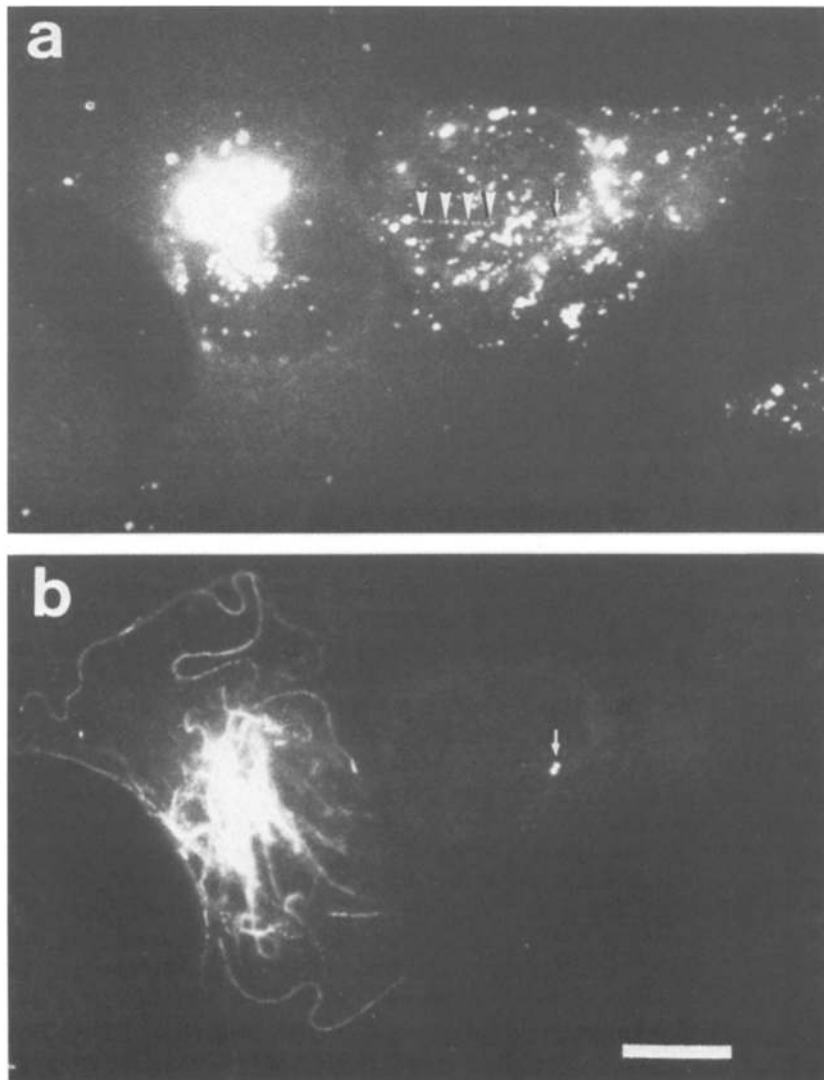
Figure 4. Lysosomes are not found aligned along microtubules predominantly containing glu-tubulin. Cells kept in culture medium were processed for double immunofluorescence staining using the monoclonal antilysosome antibody, Ly1C6 (*a*) and rabbit anti–glu-tubulin antibodies (*b*) as described in Materials and Methods. Lysosomes form linear arrays (*arrowheads* in *a*) in a cell lacking glu-tubulin containing microtubules. Arrows indicate the centrosomal region containing the centrioles, stained by anti–glu-tubulin antibodies (*b*). Bar, 10 μm.

tubulin antibodies could be detected by this time (data not shown). Cells with linear arrays of lysosomes very often lacked microtubules containing glu-tubulin and had a large number of the lysosomes scattered in the cytoplasm (Fig. 4).

Visualization of the Translocation of Endosomes and Lysosomes

NRK cells were stained with AO to visualize the movement of acidic endocytic organelles in vivo. To establish which elements of the endocytic pathway were labeled with AO we applied the following triple-staining protocol using fl-TFG, AO, and anti-LGP120 (Fig. 5). Cells were first incubated at 20 or 37°C with fl-TFG to visualize and record the endosomal compartment by VEFM (Fig. 5, *a* and *d*). Cells kept at 20 or 37°C were then quickly incubated with AO and again the pattern of labeled organelles was recorded (Fig. 5, *b* and *e*). Immediately afterwards the same cells were fixed and immunofluorescence labeling for lysosomes was performed with anti-LGP120 (Fig. 5, *c* and *f*). These experiments lead to the following conclusions. (*a*) Virtually all of the endosomes labeled at 20°C with fl-TFG were AO positive (Fig. 5, *a* and *b*; e.g., cf. *small arrowheads*). They were more

peripherally located in the cells than most of the lysosomes (Fig. 5, *a* and *c*) and very little fl-TFG was detected in the lysosome cluster in the cytocenter (Fig. 5, *a–c*, *large arrowheads*). (*b*) Internalization at 37°C for 1 h resulted in an accumulation of fl-TFG in the region of the lysosome clusters (Fig. 5, *d–f*, *arrowheads*). The overall patterns of labeling at 37°C with each of the three markers, fl-TFG, AO, and anti-LGP120, appeared very similar, although some of the labeled organelles scattered in the cytoplasm were not labeled with the lysosomal marker anti-LGP120. Such differences in the labeling pattern may be due both to movement of labeled organelles during the time span between recording in vivo and fixation of the same cells, and incomplete delivery of endocytosed fl-TFG to lysosomes within 1 h. (*c*) AO labeling did not reveal other distinct organelles than those containing fl-TFG and/or the anti-LGP120 antigen. Thus, AO labels both the endosomes and lysosomes in NRK cells, but labeling with AO does not distinguish between endosomes and lysosomes.

Movement of AO-labeled endosomes and lysosomes was recorded with VEFM using 1000–1400-fold attenuated excitation light. Virtually all the labeled organelles seen by conventional fluorescence microscopy could be detected by
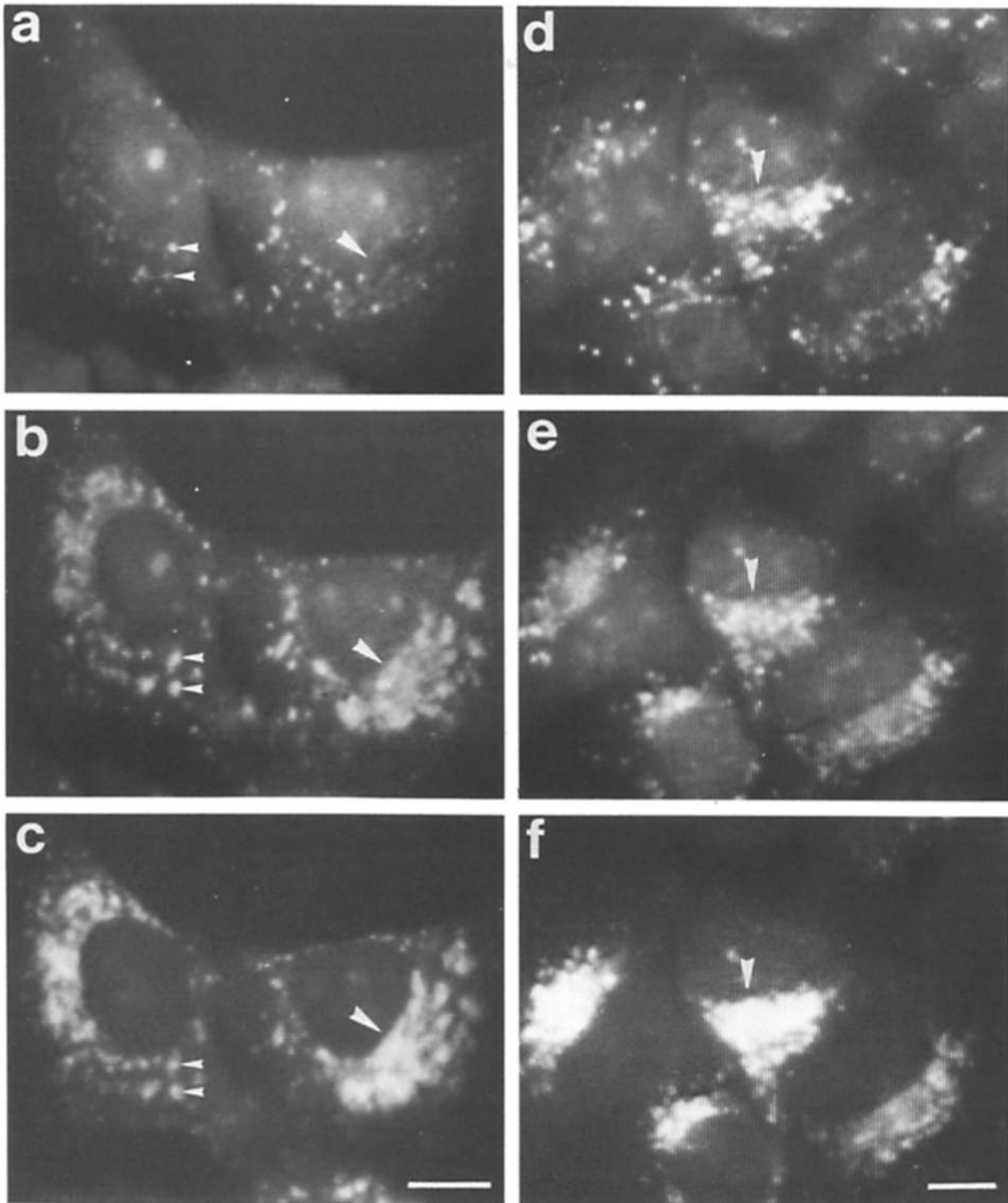
Figure 5. AO labels endosomes and lysosomes in living NRK cells. NRK cells were incubated at 20°C with fl-TFG for 30 min and for 15 min more in medium lacking the fluorescent ligand. The ligand was then visualized by VEFM (see Materials and Methods) of the living cells, which were either maintained at 20°C (*a–c*), or incubated for 1 h more at 37°C (*d–f*). Immediately after recording of the distribution of the fl-TFG (*a* and *d*), the cells were labeled with AO and the pattern of the AO-positive organelles was recorded by VEFM (*b* and *e*). Subsequently the same cells were fixed and labeled with antilysosome antibodies. The distribution of lysosomes was monitored by VEFM (*c* and *f*). Small arrowheads point to identical organelles labeled with fl-TFG, AO, and antilysosome antibodies. Large arrowheads indicate the area of clustered lysosomes. No clustering of fl-TFG-positive endocytic organelles is observed at 20°C (*a*), whereas incubation of the cells at 37°C induces accumulation of the fluorescent ligand in the region of the lysosome cluster (*d*). Bars, 10 μm.
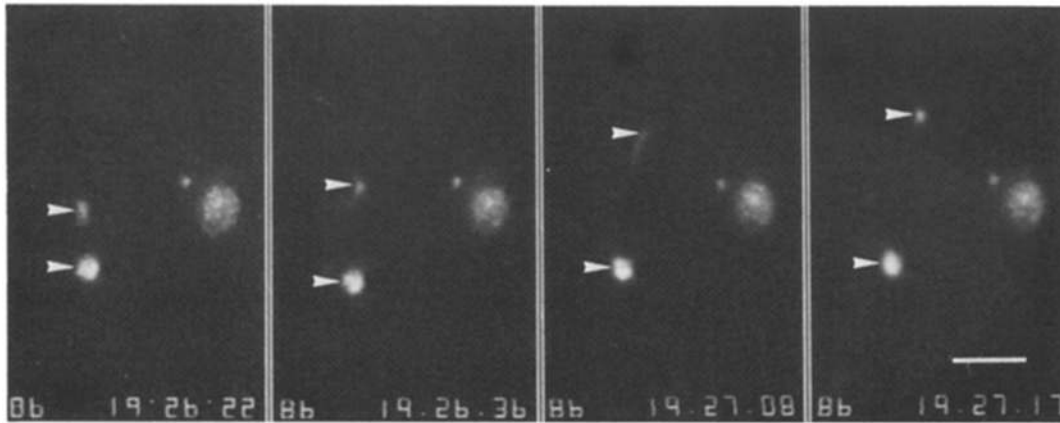
Figure 6. Visualization of saltatory movement of AO-labeled organelles. NRK cells were stained with AO and incubated at 37°C on the fluorescence microscope stage. Movement of labeled organelles was recorded by VEFM. The upper arrowhead indicates a labeled organelle moving along a linear track by two subsequent saltations. The lower arrowhead indicates an immobile AO-positive organelle. Numbers at the bottom right indicate the time in h/min/s. The recorded image of the moving organelle appears as a line because the image processing averages over 5 s (third photograph from the left at time 19:27:08). Bar, 2.5 μm.

VEFM (data not shown). These light levels did not significantly disturb translocation of endosomes or lysosomes in NRK cells continuously illuminated for up to 30 min. A typical example of saltatory translocation of an AO-positive organelle is shown in Fig. 6. The average length of such saltations observed in NRK cells was 5–10 μm, with a maximal velocity of ∼2.5 μm/s.

The Translocation and Clustering of Endosomes and Lysosomes Depends on Intact Microtubules

The tracks of moving AO-positive organelles were recorded during 10–15 min in normal or drug-treated NRK cells (Fig. 7). Typical linear saltations were observed in untreated cells (Fig. 7 A), similar to those reported by other authors (13, 21, 55). Translocation appeared to proceed both towards and away from the MTOC. About 73% of the recorded AO-labeled organelles translocated, and ∼40% moved towards the area of the MTOC (Table II). Cells which were treated with 10 μM nocodazole for 4–5 h to completely depolymerize the microtubules and to disrupt the lysosome cluster exhibited almost no saltatory movements of labeled endosomes and lysosomes; a small proportion of the organelles showed Brownian motion (4%; Fig. 7 B, Table II). However, when nocodazole-treated cells were returned to normal culture medium without nocodazole, saltatory movements of organelles resumed within 5–10 min (Fig. 7 C; for the kinetics of microtubule repolymerization see also Fig. 2). In contrast to untreated cells, >78% of the saltations were now directed towards the MTOC (Fig. 7 C, Table II). At later times (30–40 min) when reclustering of the AO-labeled organelles in the centrosomal region had occurred, bidirectional movement resumed (data not shown).

Attempts were made to colocalize the tracks of moving AO-labeled organelles with individual microtubules immediately after recording in vivo. Recorded cells were fixed and immunolabeled with antitubulin. The tracks of saltations seemed to follow microtubules (data not shown). However, due to the high density of microtubules in the areas of the cells where most movement occurred, an overlap between the tracks of moving organelles and individual microtubules could not be demonstrated unambiguously.

Translocation of Endosomes and Lysosomes Is Independent of Microfilaments and Intermediate Filaments

To study the possible role of microfilaments or intermediate filaments in translocating endosomes and lysosomes, two methods were used to specifically disrupt the organization of these cytoskeletal structures. The intermediate filaments were induced to collapse by the microinjection of a monoclonal antibody against vimentin (7A3; Kreis, T. E., unpublished results). Within 6 h after microinjection of this antibody the entire intermediate filament network was aggregated into a patch close to the nucleus (Fig. 8, *b, d,* and *f*; cf. also references 14 and 26). No individual intermediate filaments remained in the cytoplasm. By immunofluorescence labeling it was observed that lysosome clusters remained intact in cells with collapsed intermediate filaments (Fig. 8 *a*). Lysosome clusters dispersed normally after nocodazole treatment of the microinjected cells and the reclustering which occurred when the nocodazole was removed was similar to that of normal uninjected cells, (Fig. 8, *c* and *e*). Furthermore, there was characteristic saltatory movement of AO-positive organelles in the cells lacking a normal intermediate filament network. The patterns and kinetics of movements were similar to those observed in the neighboring uninjected cells (Fig. 9).

The microfilament cytoskeleton could be completely depolymerized by treating NRK cells for 1 h with 1 μM cytochalasin D. No significant effect upon saltatory movement of AO-labeled organelles could be detected after this treatment (data not shown). The dissociation of lysosome clusters after the addition of nocodazole and their subsequent reclustering after washing it out occurred normally in the cells lacking a microfilament network (data not shown). We conclude, therefore, that neither microfilaments, nor intermediate filaments are involved in the movement and clustering of endosomes and lysosomes in NRK cells.

Discussion

Receptor-mediated endocytosis is an example of directed intracellular transport. Ligands bound to specific receptors lo-
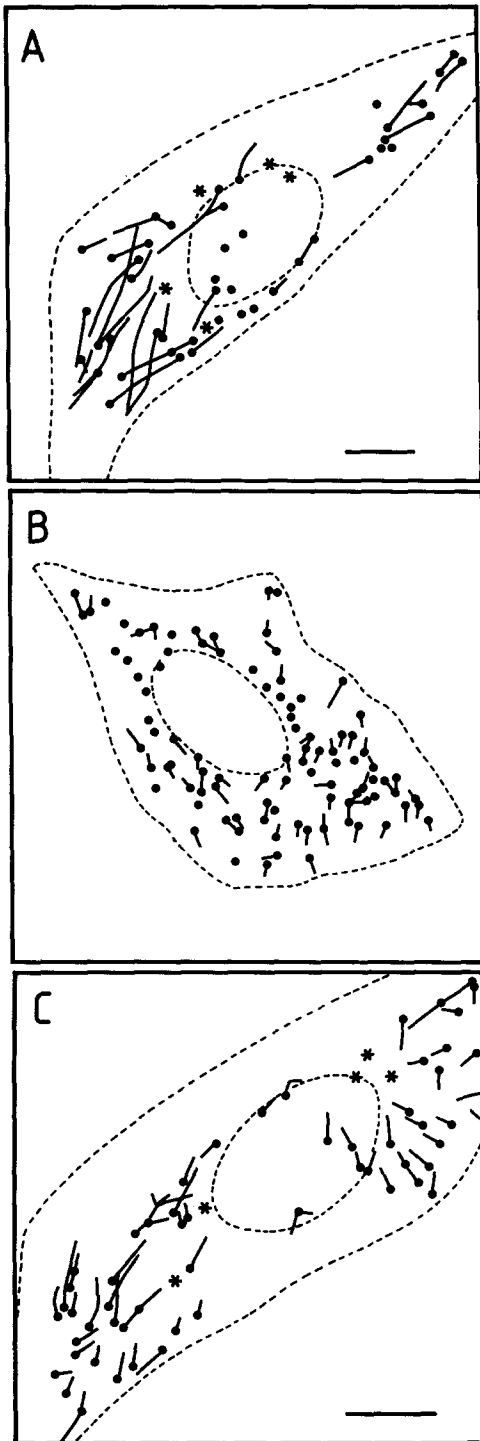
Figure 7. The effect of nocodazole on the saltatory movement of AO-labeled organelles. NRK cells, kept either in normal culture medium (*A*) or in medium containing 10 μM nocodazole for 5 h (*B-C*), were labeled with AO. Movement of labeled organelles was continuously recorded on videotape by VEFM for 10 min during incubation of the cells in H-BSA (*A* and *C*) or H-BSA containing 10 μM nocodazole (*B*). Tracks of moving organelles were manually transferred during playback of the videotape from the monitor onto transparent acetate sheets. Solid circles indicate the position of labeled organelles at the beginning of recording. Asterisks mark the position of clustered organelles. Dashed lines correspond to the cell periphery and the border of nuclei. Bars, 10 μm. *A* and *B* are shown at the same magnification.

cated on the plasma membrane are internalized and transported centripetally (13, 21, 31, 55). Immunolabeling of fixed NRK cells revealed that lysosomes accumulate in the region of the centrosomes (Fig. 1). This suggests that endocytic organelles formed at the cell periphery must ultimately migrate towards this perinuclear region. The distance from the cell periphery to the MTOC may extend to >50 μm, as is the case in motile cells where considerable endocytosis occurs, at the leading edge (22). Increasing evidence suggests that the cytoskeleton is involved in this process of endocytosis (7, 21, 38, 56). The goal of this study was to further characterize the role of cytoskeletal elements that may provide the framework for spatial positioning and translocation of endosomes and lysosomes.

In vivo analysis was required to provide further information on the involvement of cytoskeletal components in the movement of endocytic organelles. AO was used as a vital stain for endogenous acidic compartments (16, 21, 43). With an appropriate filter combination red fluorescence of AO was found exclusively in endosomes and lysosomes. These endosomes and lysosomes were identified by endocytosis of fl-TFG at 20°C (9, 33, 37) and by lysosome-specific antibodies, respectively (Fig. 5). We used VEFM to visualize the movement of AO-labeled endosomes and lysosomes in living NRK cells. At steady state the overall movement of labeled organelles consisted of randomly oriented linear saltations. Within 15 min virtually all the peripheral AO-positive organelles moved. This observation suggests that the peripheral endosomes are not spatially fixed units within the cytoplasm.

Our study confirms previous findings that the movement of endosomes and lysosomes is dependent on microtubules (13, 21, 41). However, contrary to other reports (20, 41, 52), our data strongly suggest that neither the microfilament nor the intermediate filament networks are required for the translocation or positioning of these organelles (see also reference 8). The patterns of saltatory movements of endocytic organelles in NRK cells closely resembled those observed in various other cell types (13, 21, 55, 58). The maximal velocity for translocation of AO-positive elements in NRK cells (2.5 μm/s) was also comparable to the velocities of saltations of vesicular organelles measured in a number of other cells (for reviews see 42, 44, 45), the movement of microinjected beads in tissue culture cells or axons (1, 4), and the translocation of vesicles along microtubules in vitro (3, 15, 53).

Although at steady state the movements of endosomes and lysosomes along microtubules in NRK cells appeared to be random, the following three observations suggest that under certain conditions, translocation of endosomes and lysosomes may be predominantly unidirectional, namely from the peripheral ends (the "plus" ends) of centrosomal microtubules, towards the "minus" ends associated with the MTOC (25). (*a*) Some endosomes and most of the lysosomes are usually clustered in the region of the MTOC in interphase NRK cells. (*b*) Lysosomes accumulated at the distal "minus" ends of midbody microtubules in telophase (insets Fig. 1, *e* and *f*; cf. also 10, 56) where Golgi elements also accumulate (6), in contrast to secetory granules in AtT20 cells which accumulate in the center of the mid-body (50). (*c*) Translocation of endocytic organelles is predominantly (~80%) unidirectional towards the MTOC during the initial phase of reclustering following release from nocodazole-induced de-

Table II. Quantitative Analysis of the Movement of Endosomes and Lysosomes

Treatment of NRK cells	Labeled organelles scored	Organelles moving towards MTOC		Organelles moving towards cell periphery		Ratio of inward to outward moving organelles	Moving organelles
	No.	No.	%	No.	%		%
Normal culture medium	161	62	39	55	34	1.1	73
10 µM nocodazole for 5 h	242	5	2	5	2	1	4
10 µM nocodazole for 5 h followed by incubation in normal culture medium	148	116	78	19	13	6.0	91

NRK cells were labeled with AO and movement of fluorescent organelles analyzed as described in Fig. 7. Cell culture and drug treatment is described in Fig. 1. For each condition movement of AO-positive organelles was analyzed in three different cells. The percentage of moving organelles is the percentage of all the labeled organelles which were scored.

polymerization of interphase microtubules and dispersal of the endosome/lysosome clusters.

The simplest explanation compatible with these observations is that a single translocator unit is capable of interacting with both microtubules and endosomes and lysosomes; a translocator unit which moves these organelles from the plus towards the minus ends of microtubules. It is widely accepted that the majority of the microtubules in motile cells are centrosóme nucleated (23, 25). Therefore, the density of centrosomal microtubules increases towards the MTOC, and, hence, the probability of interaction of an endosome or lysosome with a microtubule increases. Thus, the frequency of translocation of endosomes and lysosomes should increase towards the region of the centrosome and result in an accumulation of these organelles close to the MTOC. Depolymerization of interphase microtubules (induced at the onset of mitosis or by drug treatment of the cells) leads to dispersion of these organelles. Additionally, interaction of lysosomes with one another or with endosomes may cause retention of these clusters in the perinuclear region. Centrosomal microtubules have been reported to be dynamic polymers (25, 46, 48). Such a process of continuous assembly and disassembly may ensure that each area within the cytoplasm can be reached by microtubules, allowing interaction with peripherally located endosomes or lysosomes. Finally, the random movement of AO-labeled organelles observed under steady state conditions in untreated NRK cells, or at later time points after recovery of nocodazole treatment, may be caused by the presence of non–centrosome-nucleated microtubules randomly oriented in the cytoplasm (data not shown; cf. also 5 and 23). Some of these microtubules could conceivably be aligned with centrosomal microtubules, but exhibit opposite polarity. Since we postulate here that only one motor exists we suggest that a number of endosomes or lysosomes are translocated in the wrong direction along these microtubules, namely, away from the cluster in the area of the MTOC.

An alternative model to explain the translocation of endosomes and lysosomes along microtubules, both to and from the cell center, would involve the existence of two translocator units. In our opinion this model is more unlikely than the model proposed above. Proteins with activities for translocating beads in opposite directions along microtubules have been identified in squid axoplasm (54). This model

could readily explain bidirectional movement of organelles along individual microtubules. To explain the three situations discussed above, however, one would have to postulate that one of the translocator units could be transiently inactivated, or that its interaction with microtubules or organelles could be inhibited (e.g., during reclustering of organelles after nocodazole washout). Moreover, adhesive factors (as discussed above) must then be postulated to explain the clustering of these organelles in the region of the MTOC.

Why do endosomes and lysosomes accumulate in very close proximity to the Golgi complex? Does the adjacent positioning of these different compartments in the area of the MTOC facilitate intercompartmental transport? Increasing evidence suggests that some endocytosed material passes through the Golgi complex proper, or through a compartment intimately linked with the Golgi complex, before it is recycled back to the plasma membrane (11, 12, 39, 40, 47, 57). Reassembly of the Golgi complex following its dispersal after treatment of cells with nocodazole, exhibits similar kinetics to clustering of endosomes and lysosomes and depends also on the presence of repolymerized microtubules (Ho, W. C., V. J. Allan, and T. E. Kreis, manuscript in preparation). We suggest that the physiological reason for translocation of endosomes and lysosomes along microtubules is to establish, by spatial apposition in the area of the MTOC, a link between the endocytic (endosomes and lysosomes) and the exocytic (Golgi complex) membrane pathways.

Clearly, further work is required to characterize the nature of the translocator unit(s) and putative adhesive factors in the centrosomal area. An appropriate in vitro reconstituted model system, analogous to the one described by Vale et al. (54), using microtubules with defined polarity, should provide a powerful approach for the identification and biochemical characterization of the proteins involved in the process of translocation and clustering of endosomes and lysosomes in mammalian cells.
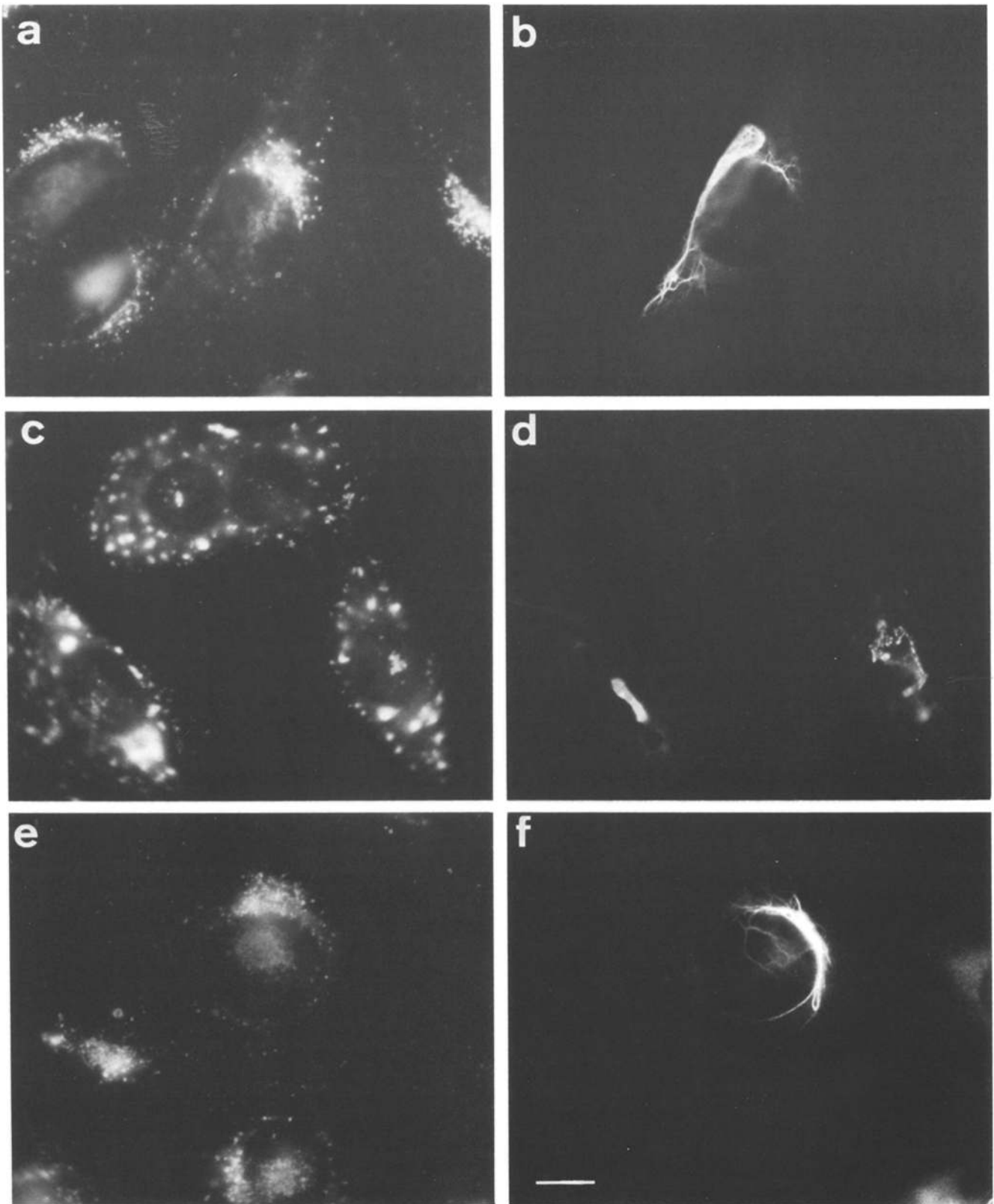
Figure 8. Reclustering of lysosomes is independent of intermediate filaments. The intermediate filament network was induced to collapse in NRK cells by microinjection of 7A3 antibodies as described in Materials and Methods. Cells were kept in normal culture medium (*a* and *b*), treated for 5 h with 10 μM nocodazole (*c* and *d*), or treated with 10 μM nocodazole for 5 h and then incubated for 1 h more in normal culture medium (*e* and *f*). Cells were then fixed and indirect double immunofluorescence labeling was carried out to visualize lysosomes (*a*, *c*, and *e*) and aggregated vimentin filaments (*b*, *d*, and *f*). Bar, 10 μM.
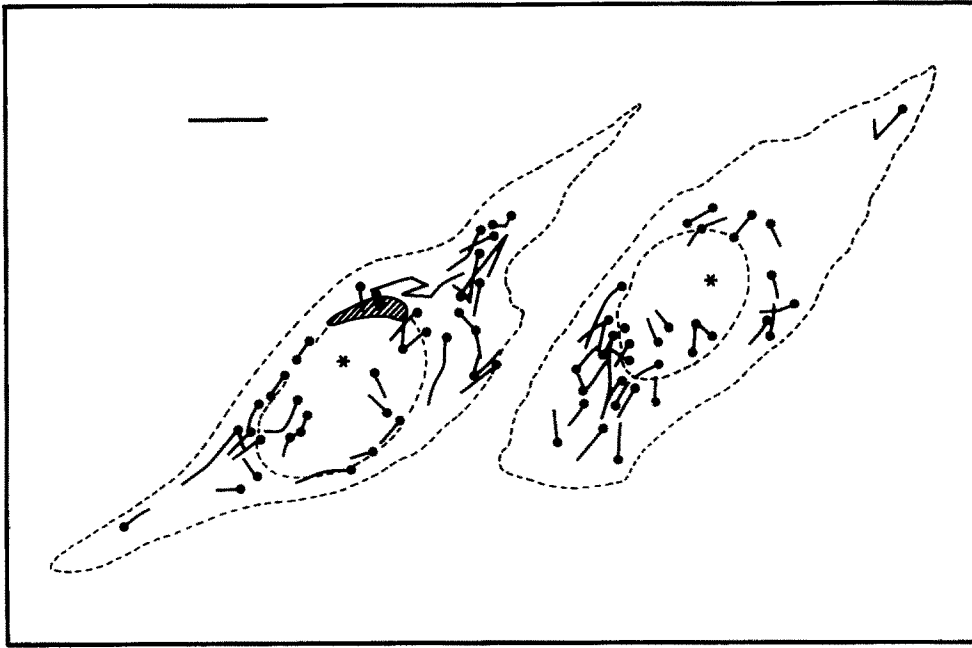
Figure 9. Saltatory movement of AO-labeled organelles is independent of intermediate filaments. NRK cells were microinjected with a rhodamine-labeled monoclonal anti-vimentin antibody (7A3) that induced, within 6 h, complete collapse of the vimentin filament network into a perinuclear aggregate (hatched area in the cell on the right). The cells were then labeled with AO. Tracks of moving organelles were recorded as described in Fig. 7. Asterisks indicate the position of clustered organelles. Bar, 10 μm.

References

1. Adams, R. J., and D. Bray. 1983. Rapid transport of foreign particles microinjected into crab axons. *Nature (Lond.).* 303:718–720.
2. Allan, V. J., and T. E. Kreis. 1986. A microtubule-binding protein associated with membranes of the Golgi apparatus. *J. Cell Biol.* 103:2229–2239.
3. Allen, R. D., D. G. Weiss, J. H. Hayden, D. T. Brown, H. Fujiwake, and M. Simpson. 1986. Gliding movement of and bidirectional transport along single native microtubules from squid axoplasm: evidence for an active role of microtubules in cytoplasmic transport. *J. Cell Biol.* 100:1736–1752.
4. Beckerle, M. C. 1984. Microinjected fluorescent polystyrene beads exhibit saltatory motion in tissue culture cells. *J. Cell Biol.* 98:2126–2132.
5. Bré, M.-H., T. E. Kreis, and E. Karsenti. 1987. Control of microtubule nucleation and stability in MDCK cells: the occurrence of noncentrosomal, stable detyrosinated microtubules. *J. Cell Biol.* 105:1283–1296.
6. Burke, B., G. Griffiths, H. Reggio, D. Louvard, and G. Warren. 1982. A monoclonal antibody against a 135K Golgi membrane protein. *EMBO (Eur. Mol. Biol. Organ.) J.* 1:1621–1628.
7. Caron, J. M., A. L. Jones, and M. W. Kirschner. 1985. Autoregulation of tubulin synthesis in hepatocytes and fibroblasts. *J. Cell Biol.* 101:1763–1772.
8. Collot, M., D. Louvard, and S. J. Singer. 1984. Lysosomes are associated with microtubules and not with intermediate filaments in cultured fibroblasts. *Proc. Natl. Acad. Sci. USA.* 81:788–792.
9. Dunn, W. A., A. L. Hubbard, and N. N. Aronson. 1980. Low temperature selectively inhibits fusion between pinocytic vesicles and lysosomes during heterophagy of ^{125}I-asialofetuin by the perfused rat liver. *J. Biol. Chem.* 255:5971–5978.
10. Euteneuer, U., and J. R. McIntosh. 1981. Structural polarity of kinetochore microtubules in PtK₁ cells. *J. Cell Biol.* 89:338–345.
11. Farquhar, M. G. 1985. Progress in unraveling pathways of Golgi traffic. *Annu. Rev. Cell Biol.* 1:447–488.
12. Fishman, J. B., and J. S. Cook. 1986. The sequential transfer of internalized, cell surface sialoglycoconjugates through the lysosomes and Golgi complex in HeLa cells. *J. Biol. Chem.* 261:11896–11905.
13. Freed, J. J., and M. M. Lebowitz. 1970. The association of a class of saltatory movements with microtubules in cultured cells. *J. Cell Biol.* 45:334–354.
14. Gawlitta, W., M. Osborn, and K. Weber. 1981. Coiling of intermediate filaments induced by microinjection of a vimentin-specific antibody does not interfere with locomotion and mitosis. *Eur. J. Cell Biol.* 26:83–90.
15. Gilbert, S. P., and R. D. Sloboda. 1984. Bidirectional transport of fluorescently labeled vesicles introduced into extruded axoplasm of squid *Loligo pealei. J. Cell Biol.* 99:445–452.
16. Gluck, S., S. Kelly, and Q. Al-Awqati. 1982. The proton translocating ATPase responsible for urinary acidification. *J. Biol. Chem.* 257:9230–9233.
17. Goldstein, J. L., M. S. Brown, R. G. W. Anderson, D. W. Russel, and W. J. Schneider. 1985. Receptor-mediated endocytosis: concepts emerging from the LDL receptor system. *Annu. Rev. Cell Biol.* 1:1–39.
18. Gundersen, G. G., M. H. Kalnoski, and J. C. Boulinski. 1984. Distinct populations of microtubules: tyrosinated and non-tyrosinated alpha tubulin are distributed differently in vivo. *Cell.* 389:779–789.
19. Helenius, A., I. Mellman, D. Wall, and A. Hubbard. 1983. Endosomes. *Trends Biochem. Sci.* 8:245–250.
20. Herman, B., and D. F. Albertini. 1982. The intracellular movement of endocytic vesicles in cultured ovarian granulosa cells. *Cell Motil.* 2:583–597.
21. Herman, B., and D. F. Albertini. 1984. A time-lapse video image intensification analysis of cytoplasmic organelle movements during endosome translocation. *J. Cell Biol.* 98:565–576.
22. Hopkins, C. R. 1986. Membrane boundaries involved in the uptake and intracellular processing of cell surface receptors. *Trends Biochem. Sci.* 11:473–477.
23. Karsenti, E., S. Kobayashi, T. Mitchison, and M. Kirschner. 1984. Role of the centrosome in organizing the interphase microtubule array: properties of cytoplasts containing or lacking centrosomes. *J. Cell Biol.* 98:1763–1776.
24. Kilmartin, J. V., B. Wright, and C. Milstein. 1982. Rat monoclonal antitubulin antibodies derived by using a new non-secreting rat cell line. *J. Cell Biol.* 93:576–582.
25. Kirschner, M., and T. Mitchison. 1986. Beyond self-assembly: from microtubules to morphogenesis. *Cell.* 45:329–342.
26. Klymkowsky, M. W. 1981. Intermediate filaments in 3T3 cells collapse after intracellular injection of a monoclonal anti-intermediate filament antibody. *Nature (Lond.).* 291:249–251.
27. Kolset, S. O., H. Tolleshaug, and T. Berg. 1979. The effects of colchicine and cytochalasin B on uptake and degradation of asialoglycoproteins in isolated rat hepatocytes. *Exp. Cell Res.* 122:159–167.
28. Kreis, T. E., and W. Birchmeier. 1982. Microinjection of fluorescently labeled proteins into living cells with emphasis on cytoskeletal proteins. *Int. Rev. Cytol.* 75:209–227.
29. Kreis, T. E., B. Geiger, and J. Schlessinger. 1982. Mobility of microinjected rhodamine actin within living chicken gizzard cells determined by fluorescence photobleaching recovery. *Cell.* 29:835–845.
30. Kreis, T. E. 1986. Microinjected antibodies against the cytoplasmic domain of vesicular stomatitis virus glycoprotein block its transport to the cell surface. *EMBO (Eur. Mol. Biol. Organ.) J.* 5:931–941.
30a. Kreis, T. E. 1987. Microtubules containing detyrosinated tubulin are less dynamic. *EMBO (Eur. Mol. Biol. Organ.) J.* 6:2597–2606.
31. Lewis, W. H. 1931. Pinocytosis. *Bull. Johns Hopkins Hosp.* 49:17–27.
32. Lewis, V., S. A. Green, M. Marsh, P. Vihko, A. Helenius, and I. Mellman. 1985. Glycoproteins of the lysosomal membrane. *J. Cell Biol.* 100:1839–1847.
33. Marsh, M., E. Bolzau, and A. Helenius. 1983. Penetration of Semliki forest virus from acidic prelysosomal vacuoles. *Cell.* 32:931–940.
34. Marsh, M. 1984. The entry of enveloped viruses into cells by endocytosis.

Biochem. J. 218:1–10.

35. Maxfield, F. R. 1985. Acidification of endocytic vesicles and lysosomes. *In* Endocytosis. I. Pastan and M. C. Willingham, editors. Plenum Publishing Corp., New York. 235–257.

36. Mellman, I., R. Fuchs, and A. Helenius. 1986. Acidification of the endocytic and exocytic pathways. *Annu. Rev. Biochem.* 55:663–700.

37. Neutra, M. R., A. Ciechanover, L. S. Owen, and H. F. Lodish. 1985. Intracellular transport of transferrin- and asialoorosomucoid-colloidal gold conjugates to lysosomes after receptor-mediated endocytosis. *J. Histochem. Cytochem.* 33:1134–1144.

38. Oka, J. A., and P. H. Weigel. 1983. Microtubule-depolymerizing agents inhibit asialo-orosomucoid delivery to lysosomes but not its endocytosis in isolated rat hepatocytes. *Biochim. Biophys. Acta.* 763:368–376.

39. Orci, L., M. Ravazzola, M. Amherdt, D. Brown, and A. Perrelet. 1986. Transport of horseradish peroxidase from the cell surface to the Golgi in insulin-secreting cells: preferential labeling of cisternae located in an intermediate position in the stack. *EMBO (Eur. Mol. Biol. Organ.) J.* 5:2097–2101.

40. Pastan, I., and M. C. Willingham. 1985. The pathway of endocytosis. *In* Endocytosis. I. Pastan and M. C. Willingham, editors. Plenum Publishing Corp., New York. 1–44.

41. Phaire-Washington, L., S. C. Silverstein, and E. Wang. 1980. Phorbol myristate acetate stimulates microtubule and 10-nm filament extension and lysosome redistribution in mouse macrophages. *J. Cell Biol.* 86:641–655.

42. Rebhun, L. I. 1972. Polarized intracellular particle transport: saltatory movements and cytoplasmic streaming. *Int. Rev. Cytol.* 32:93–137.

43. Robbins, E., P. Marcus, and N. K. Gonatas. 1964. Dynamics of acridine orange-cell interaction. II. Dye-induced changes in multivesicular bodies (acridine orange particles). *J. Cell Biol.* 21:49–62.

44. Schliwa, M. 1984. Mechanisms of intracellular transport. *Cell Muscle Motil.* 5:1–82.

45. Schroer, T. A., and R. B. Kelly. 1985. In vitro translocation of organelles along microtubules. *Cell.* 40:729–730.

46. Schulze, E., and M. Kirschner. 1986. Microtubule dynamics in interphase cells. *J. Cell Biol.* 102:1020–1031.

47. Snider, M. D., and O. C. Rogers. 1986. Membrane traffic in animal cells: cellular glycoproteins return to the site of Golgi mannosidase I. *J. Cell Biol.* 103:265–275.

48. Soltys, B. J., and G. G. Borisy. 1985. Polymerization of tubulin in vivo: direct evidence for assembly onto microtubule ends and from centrosomes. *J. Cell Biol.* 100:1682–1689.

49. Steinmann, R. M., I. Mellman, W. A. Muller, and Z. A. Cohn. 1983. Endocytosis and the recycling of plasma membrane. *J. Cell Biol.* 96:1–27.

50. Tooze, J., and B. Burke. 1987. Accumulation of ACTH secretory granules in the midbody of telophase AtT20 cells: evidence that secretory granules move anterogradely along microtubules. *J. Cell Biol.* 104:1047–1057.

51. Tuffanelli, D. L., F. McKean, D. Kleinsmith, T. K. Burnham, and M. Kirschner. 1983. Anticentromere and anti-centriole antibodies in the scleroderma spectrum. *Arch. Dermatol.* 119:560–566.

52. Valberg, P. A., and D. F. Albertini. 1985. Cytoplasmic motions, rheology and structure probed by a novel magnetic particle method. *J. Cell Biol.* 101:130–140.

53. Vale, R. D., B. J. Schnapp, T. S. Reese, and M. P. Sheetz. 1985. Movement of organelles along filaments dissociated from the axoplasm of the squid giant axon. *Cell.* 40:449–454.

54. Vale, R. D., B. J. Schnapp, T. Mitchison, E. Steuer, T. S. Reese, and M. P. Sheetz. 1985. Different axoplasmic proteins generate movement in opposite direction along microtubules in vitro. *Cell.* 43:623–632.

55. Willingham, M. C., and I. Pastan. 1978. The visualization of fluorescent proteins in living cells by video intensification microscopy (VIM). *Cell.* 13:501–507.

56. Willingham, M. C., and I. H. Pastan. 1985. Ultrastructural immunocytochemical localization of the transferrin receptor using a monoclonal antibody in human KB cells. *J. Histochem. Cytochem.* 33:54–64.

57. Woods, J. W., M. Doriaux, and M. G. Farquhar. 1986. Transferrin receptors recycle to *cis* and middle as well as *trans* Golgi cisternae in Ig-secreting myeloma cells. *J. Cell Biol.* 103:277–286.

58. Young, M. R., and P. D'Arcy-Hart. 1986. Movements and other distinguishing features of small vesicles identified by darkfield microscopy in living macrophages. *Exp. Cell Res.* 164:199–210.